

Earth effects on supernova neutrinos and their implications for neutrino parameters

Keitaro Takahashi^a and Katsuhiko Sato^{a,b}

^a*Department of Physics, University of Tokyo, 7-3-1 Hongo, Bunkyo, Tokyo 113-0033, Japan*

^b*Research Center for the Early Universe, University of Tokyo, 7-3-1 Hongo, Bunkyo, Tokyo 113-0033, Japan*

December 24, 2018

Abstract

We perform a detailed study of the Earth matter effects on supernova neutrinos with neutrino oscillation parameter LMA and small θ_{13} . The Earth effects show significant dependences on the distance which neutrinos travel in the Earth and the value of Δm^2 . We show that making use of these dependences, we can obtain implication for the value of Δm_{12}^2 by comparing the observed energy spectrum to the predicted one. When SK detect neutrinos from supernova at 10kpc which traveled through the Earth (nadir angle < 80 degree), Δm_{12}^2 can be determined with an accuracy of $\sim 2\%$ if we can obtain the original neutrino flux from the data from the other detectors which detect neutrinos directly from the supernova. In much of the neutrino-detection-time- Δm_{12}^2 plane, Δm_{12}^2 can be determined with an accuracy equal to or better than $\pm 0.5 \times 10^{-5} \text{ eV}^2$.

PACS : 14.60.Pq; 14.60.Lm; 96.40.Tv; 97.60.Bw;

Keywords : Neutrino oscillation; Supernovae; Earth effects;

1 Introduction

A type II supernova is a prodigious source of neutrinos. Almost all of the binding energy, $E_b \sim 10^{53}$ erg, is radiated away as neutrinos. These neutrinos carry information about both the core collapse process and intrinsic properties of the neutrinos. In fact, the detection of the neutrino burst from SN1987A [1, 2] induced a number of studies on these areas [3, 4, 5, 6, 7].

Neutrino oscillation, which is confirmed by the observations of solar and atmospheric neutrinos, can affect the energy spectrum of supernova neutrino drastically. Neutrinos of all flavor are produced in the high dense region of the iron core [8] and interact with matter before emerging from the supernova. The presence of non-zero masses and mixing in vacuum among various neutrino flavors results in strong matter dependent effects, including conversion from one flavor to another. Hence, the observed neutrino flux in the detectors may be dramatically different for certain neutrino flavors and for certain values of mixing parameters, due to neutrino oscillation [10, 11]. Similar matter effect occurs in the Earth, too [12, 13].

These oscillation effects on neutrino spectra depend strongly on neutrino oscillation parameters: mixing angles and mass spectrum. Some of them are firmly established but others are not. All the existing experimental results on the atmospheric neutrinos can be well described in terms of the $\nu_\mu \leftrightarrow \nu_\tau$ vacuum oscillation with mass squared difference and the mixing angle given by [14],

$$\Delta m_{atm}^2 \approx 7 \times 10^{-3} \text{eV}^2, \sin^2 2\theta \approx 1. \quad (1)$$

In contrast, for the observed ν_e suppression of solar neutrinos four solutions are still possible [15]: large mixing angle (LMA), small mixing angle (SMA), low Δm^2 (LOW), and vacuum oscillation (VO).

$$(\text{LMA}) \Delta m_{\odot}^2 \approx (1 \sim 10) \times 10^{-5} \text{eV}^2, \sin^2 2\theta_{\odot} \approx 0.7 \sim 0.95 \quad (2)$$

$$(\text{SMA}) \Delta m_{\odot}^2 \approx (4 \sim 10) \times 10^{-6} \text{eV}^2, \sin^2 2\theta_{\odot} \approx (2 \sim 10) \times 10^{-3} \quad (3)$$

$$(\text{LOW}) \Delta m_{\odot}^2 \approx (0.5 \sim 2) \times 10^{-7} \text{eV}^2, \sin^2 2\theta_{\odot} \approx 0.9 \sim 1.0 \quad (4)$$

$$(\text{VO}) \Delta m_{\odot}^2 \approx (0.6 \sim 6) \times 10^{-10} \text{eV}^2, \sin^2 2\theta_{\odot} \approx 0.8 \sim 1.0 \quad (5)$$

For θ_{13} , the mixing angle between mass eigenstate ν_1, ν_3 , only upper bound is known from reactor experiment [16] and combined three generation analysis [17]. Also the nature of neutrino mass hierarchy (normal or inverted) is still a matter of controversy.

Supernova is a completely different system from solar, atmospheric, accelerator, and reactor neutrinos in regard to neutrino energy and flavor of produced neutrinos, propagation length and so forth. Then neutrino emission from a supernova is expected to give valuable information that can not be obtained from neutrinos from other sources.

There have been some studies on the supernova neutrino as an oscillation parameter prober. Dighe et.al. [9] have studied the role the supernova neutrinos can play in the reconstruction of the neutrino mass spectrum. We have shown in our previous work [11] that the degeneracy of the solutions of the solar neutrino problem can be broken by the combination of the SK and SNO detections of a future Galactic supernova.

In this paper, we perform a detailed study of the Earth matter effects on supernova neutrinos and show that the detection of Earth matter effects allows us to probe Δm_{12}^2

more accurately than by solar neutrino observations.

2 Three-flavor formulation

In the framework of three-flavor neutrino oscillation, the time evolution equation of the neutrino wave functions can be written as follows:

$$i \frac{d}{dt} \begin{pmatrix} \nu_e \\ \nu_\mu \\ \nu_\tau \end{pmatrix} = H(t) \begin{pmatrix} \nu_e \\ \nu_\mu \\ \nu_\tau \end{pmatrix} \quad (6)$$

$$H(t) \equiv U \begin{pmatrix} 0 & 0 & 0 \\ 0 & \Delta m_{21}^2/2E & 0 \\ 0 & 0 & \Delta m_{31}^2/2E \end{pmatrix} U^{-1} + \begin{pmatrix} A(t) & 0 & 0 \\ 0 & 0 & 0 \\ 0 & 0 & 0 \end{pmatrix}, \quad (7)$$

where $A(t) = \sqrt{2}G_F n_e(t)$, G_F is Fermi constant, $n_e(t)$ is the electron number density, Δm_{ij}^2 is the mass squared differences, and E is the neutrino energy. In case of antineutrino, the sign of $A(t)$ changes. Here U is a unitary 3×3 mixing matrix in vacuum:

$$U = \begin{pmatrix} c_{12}c_{13} & s_{12}c_{13} & s_{13} \\ -s_{12}c_{23} - c_{12}s_{23}s_{13} & c_{12}c_{23} - s_{12}s_{23}s_{13} & s_{23}c_{13} \\ s_{12}s_{23} - c_{12}c_{23}s_{13} & -c_{12}s_{23} - s_{12}c_{23}s_{13} & c_{23}c_{13} \end{pmatrix}, \quad (8)$$

where $s_{ij} = \sin \theta_{ij}$, $c_{ij} = \cos \theta_{ij}$ for $i, j = 1, 2, 3 (i < j)$. We have here put the CP phase equal to zero in the CKM matrix.

In $H(t)$, the first term is the origin of vacuum oscillation, and the second term $A(t)$, which is the only time-dependent term in $H(t)$, is the origin of MSW effect.

3 Determination of neutrino oscillation parameters

In this section we summarize our previous studies on the effects of neutrino oscillation on supernova neutrino and show that future detection of neutrino from Galactic supernova allows us to break the degeneracy of the solutions of the solar neutrino problem and to probe θ_{13} .

In [11], three-flavor neutrino oscillation in the star is studied. We calculated the expected event rate and energy spectra, and their time evolution at the SuperKamiokande(SK) and the Sudbury Neutrino Observatory(SNO). For the calculations of them, we used a realistic neutrino burst model based on numerical simulations of supernova explosions [8, 18] and employed a realistic density profile based on a presupernova model [19]. The distance between the supernova and the Earth was set to 10kpc.

By solving numerically the differential equations (6) from the center of supernova to the outside of supernova, we obtained conversion probabilities $P(\nu_{\alpha \rightarrow \beta})$, i.e., probabilities that a neutrino of flavor α produced at the center of supernova is observed as a neutrino of flavor β .

We assumed normal mass hierarchy and used four sets of mixing parameters shown in table 1. Here θ_{12} and Δm_{12}^2 correspond to the solutions of solar neutrino problem and θ_{23} and Δm_{13}^2 correspond to the solution of atmospheric neutrino. The value of θ_{13} is taken to be consistent with current upper bound from reactor experiment [16]. These models are named after their values of mixing angle: LMA-L means that θ_{12} is set to be LMA of solar neutrino problem and θ_{13} is large.

We then found that when there is neutrino oscillation, neutrino spectra are harder

than those in absence of neutrino oscillation. This is because average energies of ν_e and $\bar{\nu}_e$ are smaller than those of ν_x (either of ν_μ , ν_τ , and their antineutrinos), and neutrino oscillation produces high energy ν_e and $\bar{\nu}_e$ which was originally ν_x . This feature was used as a criterion of magnitude of neutrino oscillation. We calculated the following ratio of events at both detectors:

$$R_{SK} \equiv \frac{\text{number of events at } 30 < E < 70 \text{ MeV}}{\text{number of events at } 5 < E < 20 \text{ MeV}} \quad (9)$$

$$R_{SNO} \equiv \frac{\text{number of events at } 25 < E < 70 \text{ MeV}}{\text{number of events at } 5 < E < 20 \text{ MeV}} \quad (10)$$

The plots of R_{SK} vs. R_{SNO} are shown in Fig.1. The errorbars include only statistical errors. The difference among the following three groups is clear: (1)LMA-L and LMA-S, (2)SMA-L, and (3)SMA-S and no oscillation.

In [12], the Earth effects on the energy spectra are studied using the result of [11]. For mass squared differences in table 1, the supernova neutrinos arrive at Earth in mass eigenstates. This is because neutrino eigenstates with different masses lose coherence on the way from the supernova to the Earth. Since the eigenstates of Hamiltonian in matter differ from the mass eigenstates in vacuum, supernova neutrinos begin to oscillate again in the Earth. The numbers of neutrinos of each mass eigenstates at the surface of the Earth are determined by neutrino oscillation in the supernova [12].

We analyzed numerically the time-integrated energy spectra of neutrino in a mantle-core-mantle step function model of the Earth's matter density profile. We assumed that neutrino arrived at the detectors after traveling through the Earth along its diameter. We then found that the Earth matter affects the ν_e spectrum significantly in model LMA-S

and $\bar{\nu}_e$ spectrum slightly in model LMA-S and LMA-L. In other models, there are no significant Earth effects. We concluded that we can differentiate LMA-L from LMA-S, by observing the Earth matter effect in ν_e .

Thus we can distinguish all the four models in table 1. But there are some ambiguities besides statistical errors. One is the mass of the progenitor star. Supernovae with different progenitor masses may result in different original neutrino spectra and neutrino oscillation effects. Studies on this point are now in progress. But dependence of shape of neutrino spectra on progenitor mass is not so large [20] and we would still be able to distinguish the models.

Supernova model which we use does not consider rotation of the progenitor star. In general, however, stars rotate through their lives and recent numerical simulation indicates that the rotation facilitate supernova explosion [21]. Rotation of the progenitor star can affect its density profile and the dynamics of the neutrino oscillation in supernova.

Another ambiguity is the direction of supernova. The trajectories of neutrinos change according to the location of the supernova, the position of the detector and the time t of the day at which the burst arrives at the Earth [13]. Fig 2 shows the dependence of the length d of neutrino trajectory on the time t for the three detectors, SK, SNO and LVD. d is in unit of the diameter of the Earth. Neutrino trajectory can also be described by the nadir angle θ_n of the supernova with respect to the detector. In the next section, we perform a detailed study of the Earth matter effect.

4 Detailed study of the Earth matter effect

In this section, we concentrate on model LMA-S and discuss the dependence of the Earth matter effect on the distance which neutrinos travel in the Earth and Δm_{12}^2 . But energy spectra at SK and LVD in model LMA-L are the same as in model LMA-S, since most of the events at SK and LVD are induced by $\bar{\nu}_e$ s which are influenced by the Earth matter in both LMA-L and LMA-S. The dependence on Δm_{12}^2 is expected because the oscillation length in the Earth between mass eigenstates ν_1 and ν_2 is comparable ($\sim 1000\text{km}$) to the diameter of the Earth in LMA-S model [12].

Here we use the realistic Earth density profile [22], while we used step-like model in our previous work [12]. By solving (6) along the Earth density profile numerically, we obtain conversion probability $P_{\nu_i \rightarrow \nu_\alpha}$, i.e. probability that i th mass eigenstate at the surface of the Earth is detected as neutrino of flavor α . Then combining these probabilities with the result of neutrino oscillation in supernova [11], we obtain neutrino flux and at each detector.

4.1 neutrino events at SuperKamiokande

SuperKamiokande is a water Cherenkov detector with 32,000 ton pure water based at Kamioka in Japan. The relevant interactions of neutrinos with water are as follows:



$$\nu_x + e^- \rightarrow \nu_x + e^- \quad (\text{NC}) \quad (14)$$

$$\nu_e + O \rightarrow F + e^- \quad (\text{CC}) \quad (15)$$

$$\bar{\nu}_e + O \rightarrow N + e^+ \quad (\text{CC}) \quad (16)$$

where CC and NC stand for charged current and neutral current interactions, respectively.

For the cross sections of these interactions, we refer to [23]. The appropriate detection efficiency curve is also taken into account [24]. The efficiency is 100% above 5MeV and 50% at 4.5MeV. In these interactions, the $\bar{\nu}_e p$ CC interaction [Eq.(11)] has the largest contribution to the detected events at SK. Hence the energy spectrum detected at SK (including all the reactions) is almost the same as the spectrum derived from the interaction Eq.(11) only.

4.2 neutrino event at SNO

Sudbury Neutrino Observatory(SNO) is a water Čherenkov detector based at Sudbury, Ontario. SNO is unique in its use of 1000 tons of heavy water, by which both the charged-current and neutral-current interactions can be detected. The interactions of neutrinos with heavy water are as follows,

$$\nu_e + d \rightarrow p + p + e^- \quad (\text{CC}) \quad (17)$$

$$\bar{\nu}_e + d \rightarrow n + n + e^+ \quad (\text{CC}) \quad (18)$$

$$\nu_x + d \rightarrow n + p + \nu_x \quad (\text{NC}) \quad (19)$$

$$\bar{\nu}_x + d \rightarrow n + p + \bar{\nu}_x \quad (\text{NC}) \quad (20)$$

The two interactions written in Eqs.(17) and (18) are detected when electrons emit Čerenkov light. These reactions produce electrons and positrons whose energies sensitive to the neutrino energy, and hence the energy spectra of electrons and positrons give us the information on the original neutrino flux. In this work, we mainly take into account these two charged current interactions. For the cross sections, we refer to [25]. The efficiency of detection is set to be one, because we have no information about it.

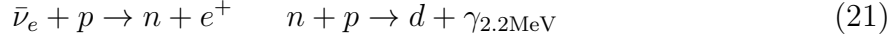
Two neutral current interactions, which produce neutrons, are detected by observing the photons emitted at the neutron absorption. Photons give energy to electrons, then the Čerenkov light from the electrons is detected. Moreover, there is a possibility to distinguish the two CC interactions by detecting neutrons because the detection of the neutron and the positron at the same time indicates the interaction in Eq.(18).

The SNO detector has also 7,000 tons of light water which can be used to detect neutrinos. This can be considered to be a miniature of SuperKamiokande (32,000 tons of light water). Then the number of events detected by light water at SNO is 7/32 of that at SuperKamiokande.

4.3 neutrino event at LVD

The Large Volume Detector (LVD) in the Gran Sasso Underground Laboratory is a ν observatory mainly designed to study low energy neutrinos from gravitational stellar collapse. LVD consists of 2 kinds of detectors, namely: liquid scintillator, for a total mass of 1840 tons, and streamer tubes for a total surface of about 7000m².

The bulk of events is due to the capture reaction:



Further, about 5% of the events are due to neutral current interactions with ^{12}C which deexcites emitting a 15.1 MeV γ . Moreover, 3% of events are due to elastic scattering of all neutrino flavours on electrons, and less than 1% to charged current interactions of ν_e and $\bar{\nu}_e$ with ^{12}C nuclei. For the cross sections, we refer to [26]. The appropriate detection efficiency curve is also taken into account [13].

4.4 nadir angle dependence of energy spectra

Fig.3, 4 and 5 shows the nadir angle dependence of neutrino spectrum at SK, SNO and LVD, respectively. Neutrino oscillation parameters are set to the values in model LMA-S except $\Delta m_{12}^2 = 2 \times 10^{-5}\text{eV}^2$. Since the oscillation lengths are comparable to the radius of the Earth, the Earth effects are strongly dependent on the nadir angle [12].

5 Δm_{12}^2 dependence of energy spectra and determination of Δm_{12}^2

5.1 method

Fig.6, 7 and 8 shows the Δm_{12}^2 dependence of energy spectrum at SK, SNO and LVD. Neutrino oscillation parameters are set to the values in model LMA-S except Δm_{12}^2 . Nadir angle is set to 0 degree. The larger Δm_{12}^2 results in higher-frequency oscillation in the energy spectra with respect to the energy. This is because the neutrino oscillation length is proportional to the inverse of Δm^2 .

As can be seen, there is significant dependence of the Earth effect on Δm_{12}^2 . Making use of this dependence, we can probe Δm_{12}^2 by the observations of the supernova neutrino spectra more accurately than by the observations of solar neutrino, if neutrino oscillation parameters are as in model LMA-S.

We assume that the direction of the supernova is given by direct optical observations or by the experimental study of the neutrino scattering on electrons [27, 28]. Comparing the observed neutrino spectra to the predicted spectra of various values of Δm_{12}^2 , we can determine the value of Δm_{12}^2 .

We performed Monte Carlo simulation to obtain the expected observed spectra and then binned according to energy resolution of each detector. For the value of the energy resolution, we refer to [13]. The energy resolution at each detector is shown in Fig.9. Energy resolution depends on neutrino energy but, for simplicity, we take constant values 4MeV, 3MeV and 6MeV for the energy resolution at SK, SNO and LVD, respectively. These values are overestimated values. Binning taking the dependence of the energy resolution on the energy into account will be discussed in the next section.

The simulated spectrum is compared to the predicted spectrum with a χ^2 method. The definition of the reduced χ^2 is,

$$\chi^2 = \frac{1}{d} \sum_{i=1}^d \frac{(N_i^{sim} - N_i^{pre})^2}{N_i^{pre}}, \quad (22)$$

where d is the number of bins and N_i^{sim} and N_i^{pre} is the simulated and predicted number of events in ith bin, respectively.

5.2 representative results

Fig.10 show the representative results of Δm_{12}^2 determination by the method described above. These are relative frequencies that the simulated spectrum based on the theoretical spectrum with $\Delta m_{12}^2 = 4 \times 10^{-5}\text{eV}^2$ is identified with the theoretical spectrum with the various values of Δm_{12}^2 . The nadir angle is set to be 0 degree at each detector and the χ^2 method is performed with the data of each detector only.

As can be seen, if the supernova occur at the direction which the nadir angle is 0 degree at SK or SNO, Δm_{12}^2 can be determined with a high accuracy $(4.00 \pm 0.07) \times 10^{-5}\text{eV}^2$ or $(4.00 \pm 0.20) \times 10^{-5}\text{eV}^2$ in case of SK and SNO, respectively. However, in case of LVD, it is difficult to determine Δm_{12}^2 . The difference in the accuracy of determination of Δm_{12}^2 is due to the difference in the properties of the detectors. Here the properties of the detectors mean the energy resolution, the detectability of ν_e and the number of events.

It is clear that high energy-resolution is advantageous for identification of the Earth effect and determination of Δm_{12}^2 . At the LVD detector, because of its low resolution, it is difficult to identify the Earth effects. Since the Earth effects are large in ν_e channel and relatively small in $\bar{\nu}_e$ channel, SK and LVD, at which most of events are $\bar{\nu}_e$, are disadvantageous. But the statistical error is very small in the energy spectrum at SK due to the large event number, ~ 10000 (10 kpc). The properties of the detectors are summarized in the Table 2.

SK is the most efficient due to its large event number and rather high energy-resolution in spite of its undetectability of ν_e . SNO is also efficient due to its high energy-resolution and detectability of ν_e although the number of events is small. Then LVD is not favorable

for detecting the Earth effects.

It should be noted that the effectiveness of determining Δm_{12}^2 depend on the value of Δm_{12}^2 itself and nadir angle. These dependences are discussed in the following subsection.

5.3 determination of Δm_{12}^2

Fig.11 shows the relative frequencies at SNO that the simulated spectrum based on the theoretical spectrum with $\Delta m_{12}^2 = 2$ (solid), 4(dashed), 6(long – dashed) $\times 10^{-5}$ eV 2 is identified with the theoretical spectrum with the various values of Δm_{12}^2 . The nadir angle is set to be 0 degree. When Δm_{12}^2 is large, the oscillation in energy spectrum become rapid and then statistical errors make it difficult to identify the Earth effect and determine Δm_{12}^2 . However at SK, its large number of events allows us to determine Δm_{12}^2 accurately irrespective of the true value of Δm_{12}^2 (Fig.12).

Fig.13 shows the relative frequencies at SNO at various nadir angles: 15 (solid), 80 (dashed) and 85 (long-dashed). The value of Δm_{12}^2 is set to be 4×10^{-5} eV 2 . Since the oscillation length of 60 MeV ν in Earth matter is ~ 6000 km [12], the Earth effects do not appear unless nadir angle is smaller than ~ 80 degree.

Now we consider the problem, 'How accurately can we determine Δm_{12}^2 when the true value of Δm_{12}^2 and the arrival time of neutrinos are given?'

As is discussed above, when the nadir angle at SK is smaller than 80 degree (time = 0 \sim 8 and 19 \sim 24 hour), the value of Δm_{12}^2 can be determined accurately using only the SK data irrespective of the value of Δm_{12}^2 in the allowed region of the solar neutrino problem. When the nadir angle is smaller than 80 degree at SNO and greater than 80 degree at SK (time = 10 \sim 19 hour), the value of Δm_{12}^2 can be determined accurately

using only the SNO data if the true value of Δm_{12}^2 is smaller than $\sim 4 \times 10^{-5} \text{ eV}^2$. However, if $\Delta m_{12}^2 > 4 \times 10^{-5} \text{ eV}^2$, the single data of SNO is not sufficient. We performed then a χ^2 method combining data of various detectors for time = 8 \sim 19 hour.

Fig.14 is the contour map of the probability that the value Δm_{12}^2 can be determined with an accuracy equal to or better than $\pm 0.5 \times 10^{-5} \text{ eV}^2$. The probability is more than 0.8 for three fourths of the time- Δm_{12}^2 plane.

6 Discussion and conclusion

In the above discussion, we overestimated the energy resolution at each detector. The overestimation is considerable especially for LVD, at which the energy resolution is significantly dependent on the energy. However, this overestimation exert little influence on the above analysis because the Earth effects are significant at high energy ($> 30 \text{ MeV}$).

In this paper, we performed a detailed study of the Earth matter effects on supernova neutrinos with neutrino oscillation parameter LMA and small θ_{13} . We showed that we can probe Δm_{12}^2 accurately by comparing the observed energy spectra to the predicted one. If SK detect supernova neutrinos which traveled through the Earth (nadir angle < 80 degree), Δm_{12}^2 can be determined with an accuracy of $\sim 2\%$. This accuracy is amazing compared to that from current solar neutrino experiments, which determine only the order of Δm_{12}^2 . In much of the time- Δm_{12}^2 plane, Δm_{12}^2 can be determined with an accuracy equal to or better than $\pm 0.5 \times 10^{-5} \text{ eV}^2$.

We assumed in this paper that the neutrino fluxes at the surface of the Earth was given. But since the original fluxes based on the numerical supernova model have some

ambiguities, we cannot use the energy spectra which we calculated in this paper to compare with the observed energy spectra in practice. Furthermore, supernova neutrino spectra depend on the mass of the progenitor star. However, we will be able to reconstruct the neutrino fluxes at the surface of the Earth from the data from the detector which detect the neutrinos directly from the supernova. Although the statistical errors then become larger and the accuracy of the determination of Δm_{12}^2 becomes worse, the Earth effects on the supernova neutrinos will still give valuable information which cannot be obtained from the other neutrino sources.

7 Acknowledgments

We would like to thank A.Suzuki for advice on cross sections of neutrino interaction in scintillator experiment. We also thank Super Kamiokande people including Y. Totsuka, Y. Suzuki, T.Kajita, M. Nakahata and Y. Fukuda for showing the most recent SK data, and fruitful discussion. This work was supported in part by Grants-in-Aid for Scientific Research provided by the Ministry of Education, Science and Culture of Japan through Research Grant No.07CE2002.

References

- [1] K. Hirata et al., Phys. Rev. Lett. **58**, 1490 (1987).
- [2] R. M. Bionta et al., Phys. Rev. Lett. **58**, 1494 (1987).
- [3] J.Arafune and M.Fukugita, Phys. Rev. Lett. **59**, 367 (1987).

- [4] H. Minakata and H. Nunokawa, hep-ph/0010240.
- [5] C. Lunardini, A. Yu. Smirnov, hep-ph/0009356.
- [6] K.Sato and H.Suzuki, Phys. Rev. Lett. **58**, 2722 (1987).
- [7] I.Goldman et al., Phys. Rev. Lett. **60**, 1789 (1988).
- [8] T.Totani, K.Sato, H.E.Dalhed and J.R.Wilson, Astrophys. J. 496 (1998) 216.
- [9] A. S.Dighe and A. Y. Smirnov, Phys. Rev. D 62 (2000) 033007.
- [10] G. Dutta, D.Indumathi, M.V.N.Murthy and G.Rajasekaran, Phys. Rev. D 61 (2000) 013009.
- [11] K.Takahashi, M.Watanabe, K.Sato and T.Totani, Phys. Rev. D accepted, hep-ph/0105204.
- [12] K.Takahashi, M.Watanabe and K.Sato, Phys. Lett. B **510**, 189 (2001).
- [13] C.Lunardini and A.Y.Smirnov, hep-ph/0106149.
- [14] Y. Fukuda et al., Phys. Rev. Lett. 82 (1999) 2644.
- [15] J.N.Bahcall, P.I.Krastev and A.Y.Smirnov, Phys. Rev. D 58 (1998) 096016.
P.I.Krastev, hep-ph/9905458.
M.C.Gonzalez-Garcia, P.C.de Holanda, C.Pena-Garay and J.W.F.Valle, hep-ph/9906469.
- [16] M.Apollonio et al.,Phys. Lett B **466**, 415 (1999).

- [17] G. L. Fogli et al. ,hep-ph/0104221; O.Yasuda and H. Minakata, hep-ph/9602386; H.Minakata and O.Yasuda, Phys. Rev. D **56**, 1692 (1997).
- [18] J. R. Wilson, R. Mayle, S. Woosley, T. Weaver, Ann. NY Acad. Sci. **470**, 267 (1986).
- [19] S. E. Woosley and T. A. Weaver, ApJ. Suppl. **101**, 181 (1995).
- [20] R.Mayle, Ph.D.Thesis, University of California (1987); R.Mayle, J.R.Wilson, and D.N.Schramm, Astrophys. J. **318**, 288 (1987).
- [21] Tetsuya M. Shimizu, Toshikazu Ebisuzaki, Katsuhiko Sato, and Shoichi Yamada, Astrophys. J. **553**, 756 (2001).
- [22] A.M.Dziewonski and D.L.Anderson, Phys.Earth.Planet.Inter. **25**(1981)297.
- [23] Y.Totsuka, Rep. Prog. Phys. **55**, 377 (1992); K.Nakamura, T.Kajita and A.Suzuki, *Kamiokande*, in *Physics and Astrophysics of Neutrino*, edited by M.Fukugita and A.Suzuki (Springer-Verlag, Tokyo, 1994).
- [24] Y.Totsuka, private communication.
- [25] S.Ying, W.C.Haxton and E.M.Henley, Phys. Rev. D **40**, 3211 (1989).
- [26] M.Fukugita, Y.Kohyama and K.Kubodera, IASSNS-AST 88/25.
- [27] J.F.Beacham and P.Vogel, Phys.Rev. **D 60** (1999) 033007.
- [28] S.Ando and K.Sato, in preparation.

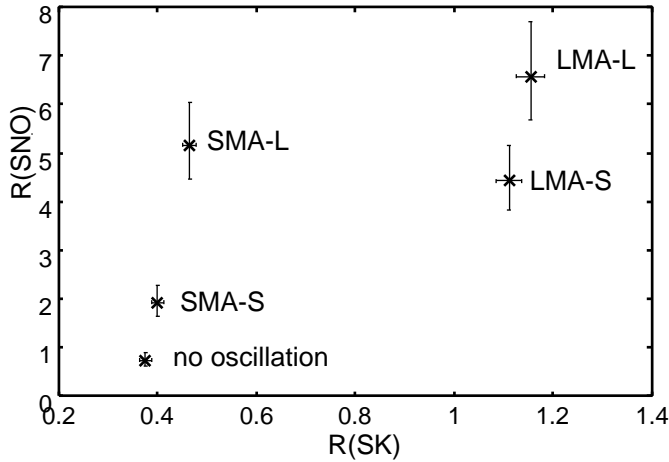


Figure 1: The plot of R_{SK} vs. R_{SNO} for all the models [11]. The error-bars represent the statistical errors.

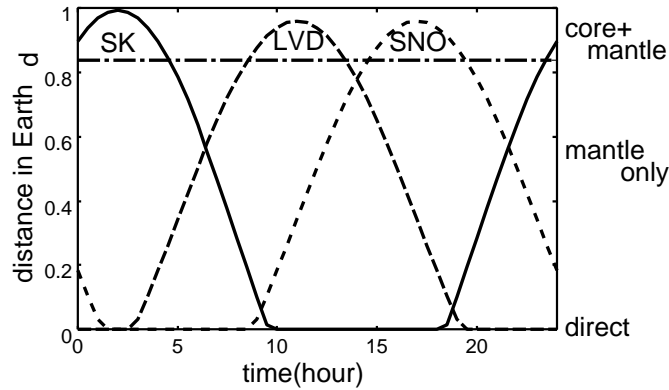


Figure 2: The distance which neutrinos travel in the Earth as functions of the arrival time of neutrino burst [13]. We assume a supernova which located in the Galactic center. We fixed $t = 0$ as the time at which the star is aligned with the Greenwich meridian.

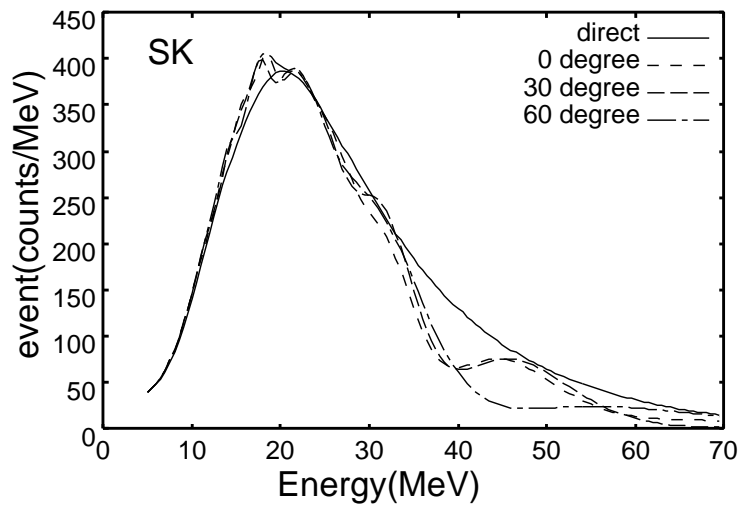


Figure 3: Nadir angle dependence of energy spectrum at SuperKamiokande. Neutrino oscillation parameters are set to the values in model LMA-S except $\Delta m_{12}^2 = 2 \times 10^{-5} \text{ eV}^2$.

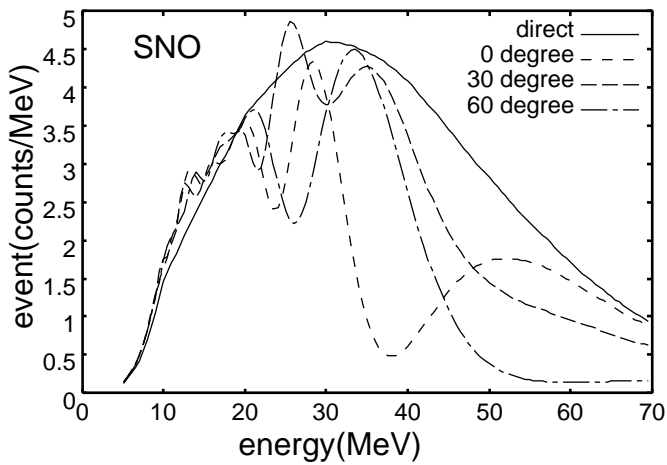


Figure 4: Nadir angle dependence of energy spectrum at SNO taking only CC events into account. Neutrino oscillation parameters are set to the values in model LMA-S except $\Delta m_{12}^2 = 2 \times 10^{-5} \text{ eV}^2$.

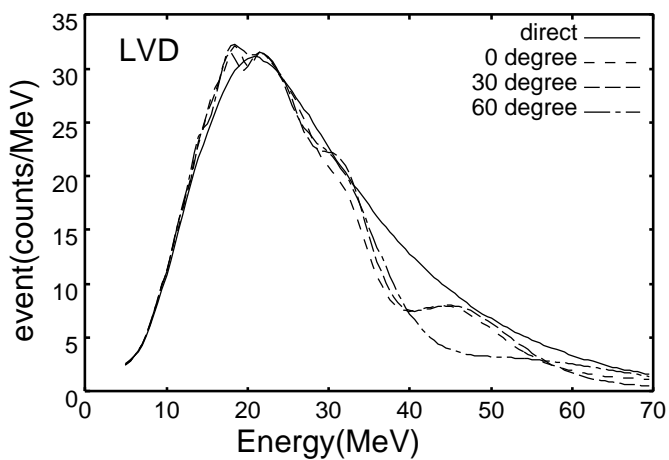


Figure 5: Nadir angle dependence of energy spectrum at LVD. Neutrino oscillation parameters are set to the values in model LMA-S except $\Delta m_{12}^2 = 2 \times 10^{-5} \text{ eV}^2$.

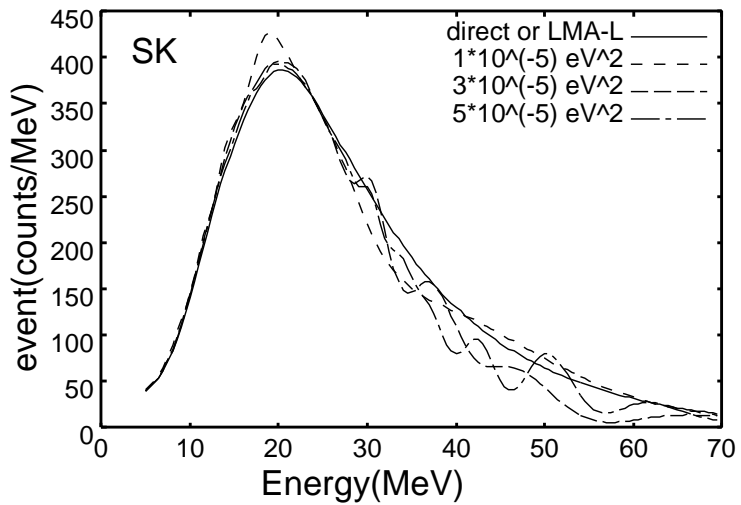


Figure 6: Δm_{12}^2 dependence of energy spectrum at SuperKamiokande. Neutrino oscillation parameters are set to the values in model LMA-S except Δm_{12}^2 . Nadir angle is set to 0 degree.

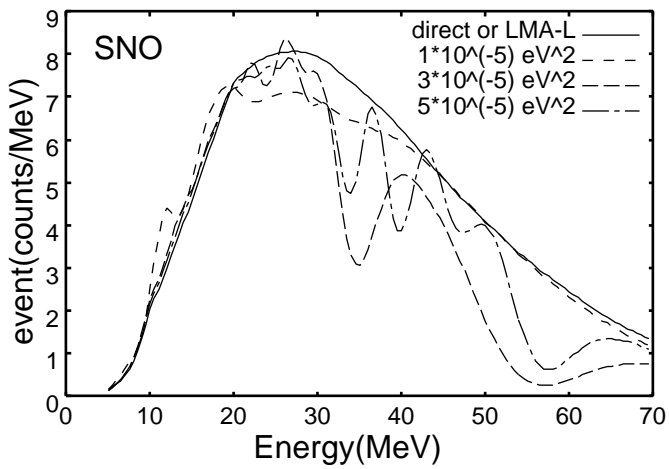


Figure 7: Δm_{12}^2 dependence of energy spectrum at SNO taking only CC events into account. Neutrino oscillation parameters are set to the values in model LMA-S except Δm_{12}^2 . Nadir angle is set to 0 degree.

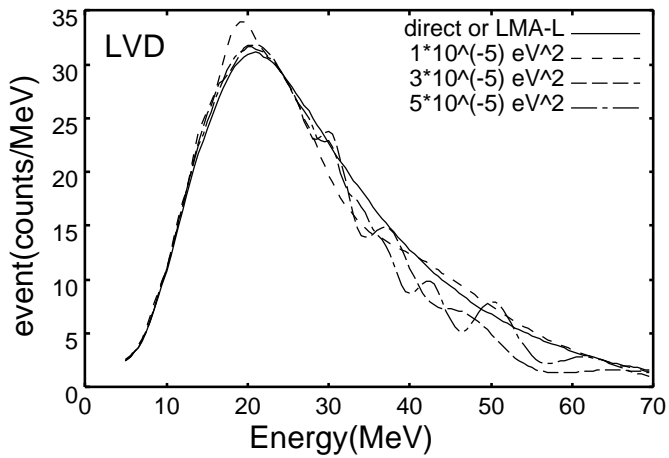


Figure 8: Δm_{12}^2 dependence of energy spectrum at LVD. Neutrino oscillation parameters are set to the values in model LMA-S except Δm_{12}^2 . Nadir angle is set to 0 degree.

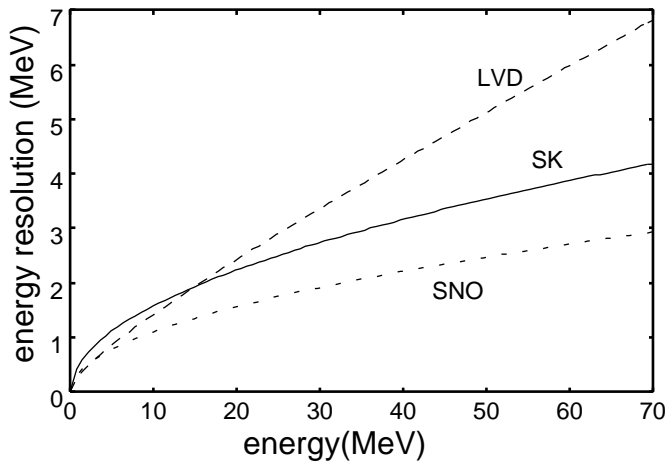


Figure 9: Energy resolution at each detector: SK (solid), SNO (dotted) and LVD (dashed) [13].

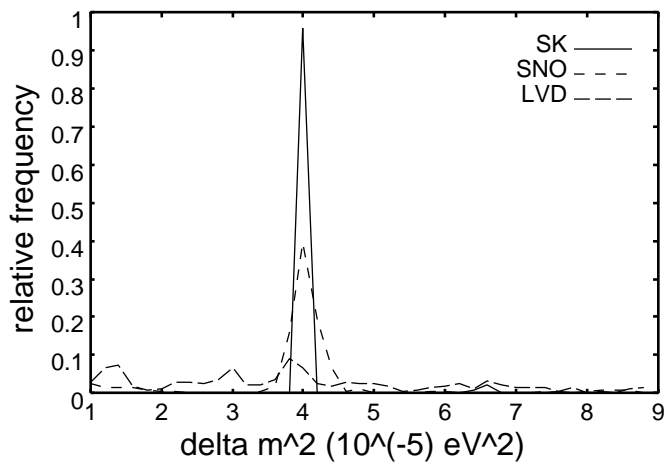


Figure 10: Relative frequencies that the simulated spectrum based on the theoretical spectrum with $\Delta m_{12}^2 = 4 \times 10^{-5} \text{ eV}^2$ is identified with the theoretical spectrum with the various values of Δm_{12}^2 . The nadir angle is set to be 0 degree at each detector and the χ^2 method is performed with the data of each detector only.

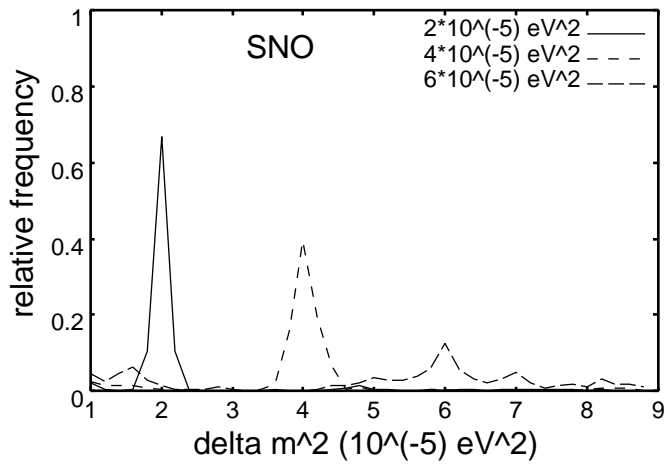


Figure 11: Relative frequencies at SNO that the simulated spectrum based on the theoretical spectrum with $\Delta m_{12}^2 = 2$ (solid), 4(dashed), 6(long – dashed) $\times 10^{-5}\text{eV}^2$ is identified with the theoretical spectrum with the various values of Δm_{12}^2 . The nadir angle is set to be 0 degree.

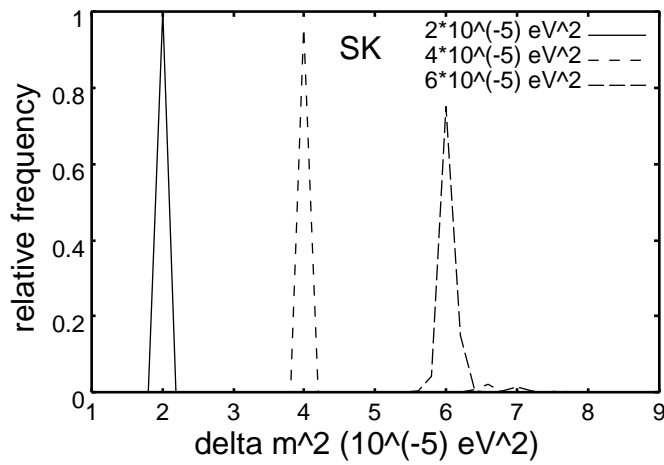


Figure 12: The same as in Fig.11 for SK.

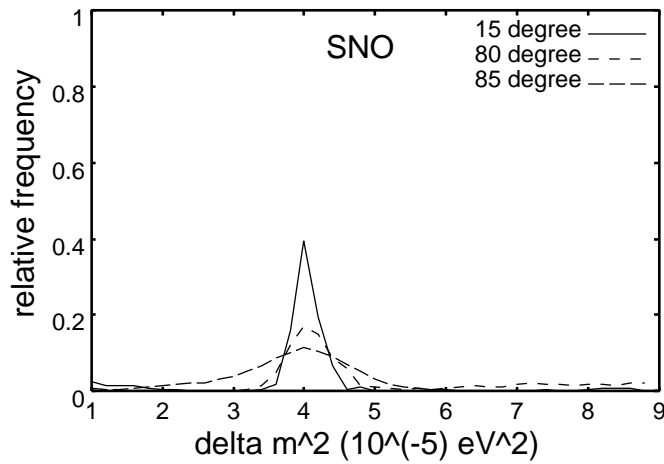


Figure 13: Relative frequencies at SNO at various nadir angles: 15 (solid), 80 (dashed) and 85 (long-dashed). The value of Δm_{12}^2 is set to be $4 \times 10^{-5} \text{ eV}^2$.

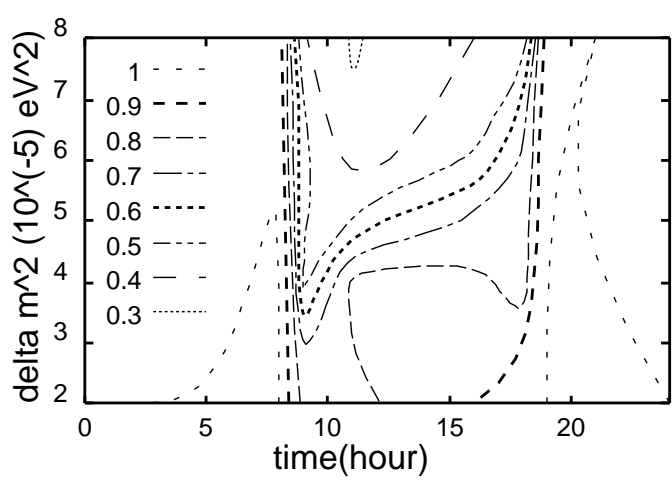


Figure 14: Contour map of the probability that the value Δm^2_{12} can be determined with an accuracy equal to or better than $\pm 0.5 \times 10^{-5} \text{ eV}^2$.

Table 1: Sets of mixing parameter for calculation

model	$\sin^2 2\theta_{12}$	$\sin^2 2\theta_{23}$	$\sin^2 2\theta_{13}$	Δm_{12}^2 (eV 2)	Δm_{13}^2 (eV 2)	ν_{\odot}	problem
LMA-L	0.87	1.0	0.043	7.0×10^{-5}	3.2×10^{-3}		LMA
LMA-S	0.87	1.0	1.0×10^{-6}	7.0×10^{-5}	3.2×10^{-3}		LMA
SMA-L	5.0×10^{-3}	1.0	0.043	6.0×10^{-6}	3.2×10^{-3}		SMA
SMA-S	5.0×10^{-3}	1.0	1.0×10^{-6}	6.0×10^{-6}	3.2×10^{-3}		SMA

Table 2: Properties of the detectors

detector	SNO	SK	LVD
main event	$\nu_e, \bar{\nu}_e$	$\bar{\nu}_e$	$\bar{\nu}_e$
number of events (10kpc)	300	10000	800
energy resolution	3 MeV	4 MeV	6 MeV